CHEMISTRY
A EUROPEAN JOURNAL

DOI: 10.1002/chem.200600633

Reactions of $Sn(NMe_2)_2$ with MPHCy: The Effects of Alkali Metal Phosphide Coupling (Cy = Cyclohexyl; M = Li, Na, K, Rb)

Paula Alvarez,[a] Felipe García,[a] Jörg P. Hehn,[a] Florian Kraus,[e] Gavin T. Lawson,[a] Nikolaus Korber,*[e] Marta E. G. Mosquera,[b] Mary McPartlin,[c] David Moncrieff,*[d] Christopher M. Pask,[a] Anthony D. Woods,[a] and Dominic S. Wright*[a]

Abstract: The reactions of the Sn^{II} base $Sn(NMe_2)_2$ with CyPHM (Cy = cyclohexyl) produce a range of products, depending primarily on the alkali metal (M) involved. The 1:3 stoichiometric reaction of $Sn(NMe_2)_2$ with CyPHNa in the presence of the Lewis base donor PMDETA (PMDETA = $(Me_2NCH_2CH_2)_2NMe$) gives $[(Na{\cdot}PMDETA)_2\{Sn(\mu\text{-}PCy)\}_3]$ (**3**), containing the electron-deficient $[\{Sn(\mu\text{-}PCy)\}_3]^{2-}$ dianion. Natural bond order (NBO) and electron localisation function (ELF) calculations show that this species is described most appropriately by a two-electron, three-centre Sn_3 bonding model. Evidence that **3** results from phosphide coupling is provided by the 1:1 reaction of $Sn(NMe_2)_2$ with CyPHNa in the presence of PMDETA, which gives **3** and trace amounts of $(Na{\cdot}PMDETA)_2[\{Sn(\mu\text{-}PCy)\}_2(\mu\text{-}PCyPCy)]$ (**4**) (containing one $PCyPCy^{2-}$ dianion). Greater extents of phosphide coupling are observed as the size of the Group 1 metal is increased. Thus, the 1:3 reaction of $Sn(NMe_2)_2$ with CyPHK in THF gives the co-crystalline product $\{(K{\cdot}2\,THF)_2[\{Sn(\mu\text{-}PCyPCy)\}_2(\mu\text{-}PCy)]\}_{0.9}\{(K{\cdot}2\,THF)_2[\{Sn(\mu\text{-}PCy)\}_2(\mu\text{-}PCyPCy)]\}_{0.1}$ (**5**) (containing $[\{Sn(\mu\text{-}PCyPCy)\}_2(\mu\text{-}PCy)]^{2-}$ and $[\{Sn(\mu\text{-}PCy)\}_2(\mu\text{-}PCyPCy)]^{2-}$ dianions), whereas the analogous reaction of $Sn(NMe_2)_2$ with RbPHCy gives $[Rb{\cdot}PMDETA\{(CyP)_3SnP(H)Cy\}]$ (**6**) (containing a cyclic $\{(CyP)_3Sn\}$ unit).

Keywords: cage compounds · main group elements · phosphorus · structure elucidation · tin

Introduction

Recently we have shown that reactions of Group 15 dimethylamido reagents $E(NMe_2)_3$ (E = As, Sb) with metalated primary phosphines (RPHM; M = alkali metal) result in the formation of Zintl compounds.[1] This process occurs by coupling of the phosphide units of the initially formed heterometallic phosphide cages, such as $[Li_6\{Sb(PR)\}_3]$ (R = Cy,[2] *t*Bu[3]). The isolation of cyclic phosphines $[RP]_m$ along with the Zintl compounds suggests that the formation of stable P–P single bonds provides the thermodynamic driving force for these "cage-to-alloy" reactions. Further mechanistic detail is revealed by the isolation of the heterocyclic anions $[(RP)_nE]^-$ ($n = 3$ or 4) as intermediates in this process.[4] The latter can be regarded as being responsible for the delivery of the metal centres. The mechanism of E–E bond formation appears to involve coupling of the $[(RP)_nE]$ units prior to elimination of $[RP]_m$ (and the formation of the polyatomic E_7^{3-} ions (Scheme 1)).[3,4b]

Two important reactivity trends are apparent from studies of Group 15 phosphides:[1] 1) the presence of aromatic substituents in the phosphine encourages formation of Zintl compounds and, 2) the tendency for P–P bond formation

[a] P. Alvarez, Dr. F. García, J. P. Hehn, Dr. G. T. Lawson, Dr. C. M. Pask, Dr. A. D. Woods, Dr. D. S. Wright
Chemistry Department, Cambridge University
Lensfield Road, Cambridge CB2 1EW (UK)
Fax: (+44) 1223-336-362
E-mail: dsw1000@cus.cam.ac.uk.

[b] Dr. M. E. G. Mosquera
Departamento de Quimica Inorganica
Universidad de Alcala, Madrid (Spain)

[c] Prof. M. McPartlin
Department of Health and Biological Sciences
London Metropolitan University, London N7 8DB (UK)

[d] Dr. D. Moncrieff
School of Computational Science & Information Technology
Florida State University, Tallahassee, FL 32306–4120 (USA)

[e] Dr. F. Kraus, Prof. N. Korber
Institut für Anorganische Chemie
Universität Regensburg (Germany)
Fax: (+49) 941-943-1812
E-mail: nikolaus.korber@chemie.uni-regensburg.de

Supporting information for this article is available on the WWW under http://www.chemeurj.org/ or from the author.

WILEY InterScience DISCOVER SOMETHING GREAT
© 2007 Wiley-VCH Verlag GmbH & Co. KGaA, Weinheim

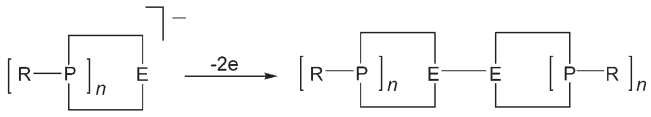

Scheme 1.

and the production of Zintl compounds increases as Group 1 is descended. Recent studies of the reactions of $Sn(NMe_2)_2$ have shown that the first of these reactivity trends is also observed for Group 14. For example, the reactions of $Sn(NMe_2)_2$ with lithiated aliphatic phosphines (RPHLi) (1:3 equivalents) give the cage complexes $(Li{\cdot}THF)_4[\{[Sn(\mu\text{-}PR)]_2(\mu\text{-}PR)\}_2]$ (R = Cy (**1a**), *t*Bu (**1b**)), containing metallacyclic $[\{Sn(\mu\text{-}PR)\}_2(\mu\text{-}PR)]_2^{4-}$ tetraanions (Scheme 2).[5] However, the reaction of $Sn(NMe_2)_2$ with the aromatic

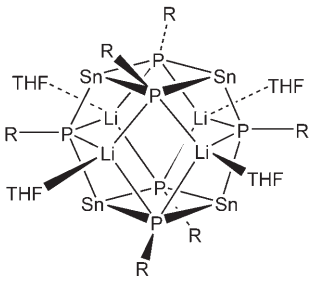

Scheme 2. Structure of the cages **1a** (R = Cy) and **1b** (R = *t*Bu).

phosphide MesPHLi (1:2–3 equivalents) gave $(Li{\cdot}TMEDA)_2[Sn(\mu\text{-}PMes)\}_2(\mu\text{-}PMesPMes)]$ (Mes = 2,4,6-$Me_3C_6H_2$) (**2**) (Scheme 3) in which partial coupling of the MesP units has occurred within the $[\{Sn(\mu\text{-}PMes)\}_2(\mu\text{-}PMesPMes)]^{2-}$ dianion.[5]

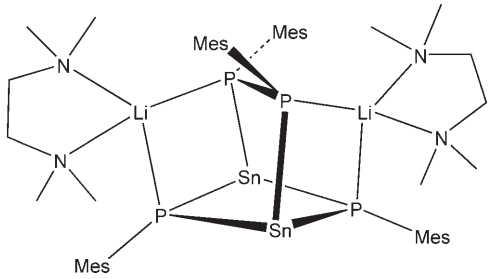

Scheme 3. Structure of **2**.

We present here studies of the reactions of $Sn(NMe_2)_2$ with the heavier alkali metal cyclohexyl phosphides [MPHCy] (M = Na, K, Rb). In a recent communication we showed that the reaction between $Sn(NMe_2)_2$ and NaPHCy in the presence of the Lewis base donor PMDETA [PMDETA = $(Me_2NCH_2CH_2)_2NMe$)] gives $[(Na{\cdot}PMDETA)_2\{Sn(\mu\text{-}PCy)\}_3]$ (**3**), containing an electron-deficient $[\{Sn(\mu\text{-}PCy)\}_3]^{2-}$ ion (Figure 1).[6] We present here

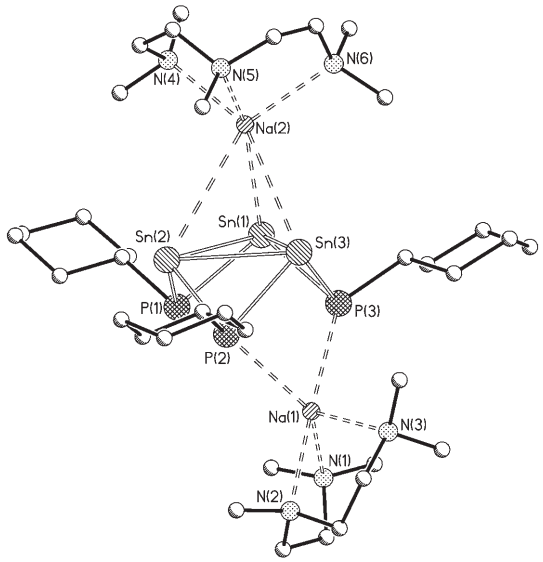

Figure 1. Structure of **3**.[6]

a full account of our work in this area, including full details of theoretical calculations of the bonding in the anion of **3**, and the syntheses and structures of the new complexes $(Na{\cdot}PMDETA)_2[\{Sn(\mu\text{-}PCy)\}_2(\mu\text{-}PCyPCy)]{\cdot}1.5$ toluene (**4**·1.5 toluene), $\{(K{\cdot}2\,THF)_2[\{Sn(\mu\text{-}PCyPCy)\}_2(\mu\text{-}PCy)]\}_{0.9}\{(K{\cdot}2\,THF)_2[\{Sn(\mu\text{-}PCy)\}_2(\mu\text{-}PCyPCy)]\}_{0.1}$ (**5**) and [Rb·PMDETA·THF{$(CyP)_3SnP(H)Cy$}] (**6**·THF).

Results and Discussion

Our primary aim at the beginning of these studies was to explore the potential links between the reaction characteristics of Group 14 and Group 15 dimethylamido reagents with alkali metal primary phosphides [MPHR]. As noted in the introduction, the different results observed in the reactions of aliphatic primary phosphides of lithium (LiPHR; R = Cy, *t*Bu) and aromatic primary phosphides (i.e., MesPHLi) with $Sn(NMe_2)_2$ suggest that a similar reactivity trend is likely as far as the organic substituent is concerned.[5] However, too little data has been available so far to allow mechanisms to be advanced. The heavier alkali metal cyclohexyl phosphides (MPHCy; M = Na–Rb) are readily obtained by the in situ reactions of MCH_2Ph with $CyPH_2$ in toluene. The organoalkali metal precursors [MCH_2Ph] were prepared by reactions of *t*BuOM with *n*BuLi in toluene. We have shown previously in the study of the reactions of RPHLi with $Sn(NMe_2)_2$ that a 3:1 stoichiometry of LiPHCy to $Sn(NMe_2)_2$ leads to the cleanest reactions and to the highest yields of the products obtained.[5] For this reason the same stoichiometry was used in our initial investigations of the reactions of the MPHCy (M = Na–Rb) with $Sn(NMe_2)_2$. The reactions of a range of MPHCy with $Sn(NMe_2)_2$ in toluene (24 h) gave orange or orange-red powders as the products. These were insoluble in non-polar organic solvents. However, removal

 © 2007 Wiley-VCH Verlag GmbH & Co. KGaA, Weinheim

of the toluene under vacuum and addition of THF and/or a bi- or tridentate nitrogen Lewis base donor allowed some or all of the solids to be dissolved. Filtration of the suspensions produced clear solutions from which crystalline products were isolated. The complexes $[(Na{\cdot}PMDETA)_2\{Sn(\mu\text{-}PCy)\}_3]$ (**3**), $\{(K{\cdot}2THF)_2[\{Sn(\mu\text{-}PCyPCy)\}_2(\mu\text{-}PCy)]\}_{0.9}\{(K{\cdot}2THF)_2[\{Sn(\mu\text{-}PCy)\}_2(\mu\text{-}PCyPCy)]\}_{0.1}$ (**5**) and $[Rb{\cdot}PMDETA{\cdot}THF\{(CyP)_3SnP(H)Cy\}]$ (**6**·THF) were obtained by using this procedure (Scheme 4) (see Experimental Section). ^{31}P NMR spectroscopic investigations of the reaction solutions from which **3** and **5** are obtained revealed the cyclophosphane $[CyP]_4$ and unreacted [MPHCy] are also present. In the case of the reaction producing **6**, however, ^{31}P NMR spectroscopic studies show that only **6** and $[CyP]_4$ are formed. Varying the stoichiometry of these reactions (between 3:1 and 1:1, MPHCy:$Sn(NMe_2)_2$) did have some effect on the distribution of products. The 1:1 reaction of NaPHCy with $Sn(NMe_2)_2$ in the presence of PMDETA also gave **3** as the major product. However, using this stoichiometry, complex **3** is contaminated with a minor quantity of $[(Na{\cdot}PMDETA)_2\{Sn(\mu\text{-}PCy)\}_2(\mu\text{-}PCyPCy)]{\cdot}1.5$ toluene (**4**·1.5 toluene) (estimated to be less than 5% from inspection).

Complex **4**·1.5 toluene was only characterised by X-ray crystallography, owing to the fact that it is obtained as a minor impurity in **3**. Although **6** is formed almost quantitatively by the reaction of RbPHCy with $Sn(NMe_2)_2$ in the presence of PMDETA (as a red powder, contaminated with $[CyP]_4$), its low solubility in THF resulted in only low yields of pure, crystalline samples of the complex being isolated by storage of the filtrate at low temperature. Despite repeated attempts, satisfactory elemental analysis for **6** could not be obtained. However, unit cell analysis and ^{31}P NMR spectroscopic studies of crystals from several separate reactions all showed that **6** is formed reproducibly. The room-temperature ^{31}P NMR spectrum of **6** in THF is particularly diagnostic. The central P atom within the P_3Sn ring unit [P(1)] appears as a triplet ($\delta = 74.0$ ppm), the terminal P atoms of this unit [P(2)] is observed as a double-doublet ($\delta = -10.7$ ppm) and the terminal CyPH P centre [P(3)] appears as a triplet ($\delta = -3.4$ ppm). The coupling constant between the two P centres of the P_3Sn ring ($J_{P(2),P(1)} = 162.0$ Hz) is typical of $^1J_{P,P}$ coupling constants,[7] while the value found across the CyPHSnP fragment is considerably smaller ($J_{P(2),P(3)} = 87.6$ Hz), as would be expected for a $^2J_{P,P}$ coupling constant. In contrast, the room-temperature ^{31}P NMR spectrum of **5** in THF shows a complicated series of overlapping multiplets in the region $\delta = -127.0$ to -222.2 ppm, which change with concentration and temperature, suggesting that a number of solution species are present in equilibrium. However, no obvious (first-order) resonances for the *intact* $[\{Sn(\mu\text{-}PCyPCy)\}_2(\mu\text{-}PCy)]^{2-}$ and $[\{Sn(\mu\text{-}PCy)\}_2(\mu\text{-}PCyPCy)]^{2-}$ dianions present in **5** could be discerned. Presumably owing to a combination of their low solubilities (even in THF solvent) and to fast relaxation, we have not been able to observe ^{119}Sn NMR resonances for complex **3** or **6**. This is despite the fact that $^{119,117}Sn$ NMR satellites are observed for the ion-paired and separated $[\{Sn(\mu\text{-}PCy)\}_3]^{2-}$ ion in the ^{31}P NMR spectrum of **3** in DMSO. In the case of **5**, only a sharp singlet ($\delta = -1540.0$) is observed, the chemical shift of which is characteristic of Sn^{II}.

Details of the structural solutions and refinements of the new complexes **4**·1.5 toluene, **5** and **6**·THF are given in Table 1. Key bond lengths and angles for **4**·1.5 toluene, **5** and **6**·THF are listed in Tables 2–4, respectively.

The crystallographic study of **4** shows that it is an ion-paired complex $(Na{\cdot}PMDETA)_2[\{Sn(\mu\text{-}PCy)\}_2(\mu\text{-}CyPCy)]$, resulting from the association of the bicyclic Sn^{II} phosphide dianion $[\{Sn(\mu\text{-}PCy)\}_2(\mu\text{-}PCyPCy)]^{2-}$ with two PMDETA-coordinated Na^+ ions (Figure 2). In addition, three half toluene molecules are present for each molecule of **4** in the crystal lattice. The structural arrangement of the dianion in **4**, composed of two Sn^{II} centres bridged by two μ-PCy groups and one PCy–PCy group, is similar to that previously reported in the Li^+ complex $(Li{\cdot}TMEDA)_2[Sn(\mu\text{-}PMes)\}_2(\mu\text{-}PMesPMes)]$ (**2**).[5] Of particular note in comparison to **2** and **4** is the formation of the Sn^{II} phosphide $(Ca{\cdot}2THF)_2[(Me_3Si)PSn(\mu\text{-}PSiMe_3)]_2$ in the reaction of $[Ca\{P(SiMe_3)_2\}_2]$ with $SnCl_2$.[8] The $[(Me_3Si)PSn(\mu\text{-}PSiMe_3)]_2^{4-}$ tetraanion of the latter can be regarded as related to the $[\{Sn(\mu\text{-}PR)\}_2\{\mu\text{-}P(R)P(R)\}]^{2-}$ dianions of **2** and **4** by 2e reduction and cleavage of the P–P bonds (Scheme 5).

The P-Sn-P angles in **4** (78.0(1)–95.4(1)°) closely match those found in the previously reported complex $(Li{\cdot}TMEDA)_2[\{Sn(\mu\text{-}PMes)\}_2(\mu\text{-}PMesPMes)]$ (**2**) (Scheme 3; range 75.75(3)–94.71(3)°).[5] The pyramidal geometries of the metal centres in both complexes are symptomatic of the presence of stereochemically active lone pairs, pointing *exo*

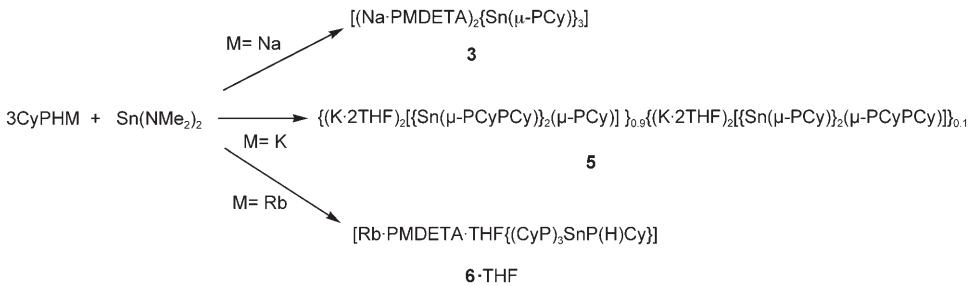

Scheme 4.

 © 2007 Wiley-VCH Verlag GmbH & Co. KGaA, Weinheim

Table 1. Details of the data collections and refinements for **4**·1.5 toluene, **5** and **6**·THF.

Compound[a]	**4**·1.5 toluene	**5**	**6**·THF
formula	$C_{52.5}H_{102}N_6Na_2P_4Sn_2$	$C_{90.80}H_{171.80}K_4O_8P_{9.80}Sn_4$	$C_{37}H_{76}N_3OP_4RbSn$
fw	1224.64	2326.35	907.05
crystal system	monoclinic	triclinic	orthorhombic
space group	$P2_1/c$	$P\bar{1}$	*Ibam*
unit cell dimensions			
a [Å]	16.1358(6)	13.753(3)	22.333(5)
b [Å]	16.7770(8)	14.229(3)	20.524(4)
c [Å]	27.0531(12)	17.025(3)	21.685(4)
α [°]	–	95.72(3)	–
β [°]	98.3960(10)	99.42(3)	–
γ [°]	–	117.83(3)	–
crystal size	0.23×0.21×0.18	0.18×0.12×0.10	0.18×0.18×0.05
μ [mm^{-1}]	0.821	1.197	1.643
ρ_{calcd} [Mg m^{-3}]	1.123	1.357	1.212
Z	4	1	8
V [Å^3]	7245.1(5)	2846.7(10)	9940(3)
Θ-range	3.52–17.38	3.63–25.04	4.18–21.00
independent reflns.	4242	9867	2675
R_{int}	0.027	0.038	0.048
R indices [$I>2\sigma(I)$]			
$R1$	0.062	0.049	0.075
$WR2$	0.175	0.113	0.210
R indices (all data)			
$R1$	0.067	0.062	0.087
$WR2$	0.179	0.120	0.222
goodness-of-fit	1.066	1.078	1.003
largest peak/hole	1.053/−0.492	0.084/−0.629	1.354/−0.865

[a] Data in common; $T=180(2)$ K, $\lambda=0.71073$ Å.

Table 2. Selected bond lengths [Å] and angles [°] for **4** in the toluene solvate **4**·1.5 toluene.

Sn(1)−P(1)	2.622(3)	P(2)−Na(2)	2.858(5)
Sn(1)−P(2)	2.600(3)	P(4)−Na(2)	2.959(5)
Sn(1)−P(3)	2.614(3)	Na(1)−N(1)	2.43(1)
Sn(2)−P(1)	2.610(3)	Na(1)−N(2)	2.48(1)
Sn(2)−P(2)	2.612(3)	Na(1)−N(3)	2.47(1)
Sn(2)−P(4)	2.621(3)	Na(2)−N(4)	2.47(1)
P(3)−P(4)	2.194(4)	Na(2)−N(5)	2.53(1)
P(1)−Na(1)	2.844(5)	Na(2)−N(6)	2.45(1)
P(3)−Na(1)	2.917(5)		
P(1)-Sn(1)-P(2)	91.0(1)	Sn(1)-P(2)-Sn(2)	85.81(9)
P(1)-Sn(1)-P(3)	80.0(1)	Sn(1)-P(3)-P(4)	100.5(1)
P(2)-Sn(1)-P(3)	95.1(1)	Sn(2)-P(4)-P(3)	100.8(1)
P(1)-Sn(2)-P(2)	91.0(1)	P(1)-Na(1)-P(3)	71.5(1)
P(1)-Sn(2)-P(4)	95.4(1)	P(2)-Na(2)-P(4)	69.9(1)
P(2)-Sn(2)-P(4)	79.10(9)		
Sn(1)-P(1)-Sn(2)	85.40(9)	fold about P(1)···P(2) of P(1)-Sn(1)-P(2)-Sn(2)	151.5

Table 3. Selected bond lengths [Å] and angles [°] for **5a** in the mixed crystal **5**.[a]

Sn(1)−P(1)	2.615(2)	K(1)−P(1)	3.290(2)
Sn(1)−P(3)	2.600(2)	K(1)−P(3)	3.438(2)
Sn(1)−P(5)	2.573(1)	K(1)−O(1S,1T)	mean 2.70
Sn(1)−K(1C)	3.726(2)	K(2)−P(4)	3.353(2)
Sn(2)−P(2)	2.601(2)	K(2)−P(5)	3.280(2)
Sn(2)−P(4)	2.600(2)	K(2)−O(2S,2T)	mean 2.67
Sn(2)−P(5)	2.604(2)	P(1)−P(2)	2.200(2)
Sn(2)−K(2C)	3.674(2)	P(3)−P(4)	2.214(2)
P(1)-Sn(1)-P(3)	91.35(5)	Sn(1)-P(1)-P(2)	111.45(8)
P(1)-Sn(1)-P(5)	99.60(6)	Sn(2)-P(2)-P(1)	108.29(7)
P(3)-Sn(1)-P(5)	92.87(5)	Sn(1)-P(3)-P(4)	105.97(7)
P(2)-Sn(2)-P(4)	105.46(5)	Sn(2)-P(4)-P(3)	107.66(6)
P(2)-Sn(2)-P(5)	102.11(5)	P(1)-K(1)-P(3)	67.31(5)
P(4)-Sn(2)-P(5)	81.59(5)	P(4)-K(2)-P(5)	61.65(4)
Sn(1)-P(5)-Sn(2)	100.40(5)		

[a] Symmetry transformations used to generate equivalent atoms here, and in Figure 4; A: $-x$, $-y+1$, $-z+1$; B: x, y, $1+z$; C: $-x$, $-y+1$, $-z+2$. Only bond lengths for the major component are given.

Table 4. Selected bond lengths [Å] and angles [°] for **6**·THF.[a]

Sn(1)−P(2)	2.615(2)	N(1)−Rb(1)	3.00(1)
Sn(1)−P(3)	2.599(4)	N(2)−Rb(1)	2.95(1)
P(1)−P(2)	2.212(3)	P(3)···O(1S)	3.21(2)
P(2)−Rb(1)	3.436(2)	H(3)···O(1S)	1.98(3)
P(3)−Rb(1)	3.362(4)		
P(2)-Sn(1)-P(2A)	74.76(9)	P(2)-P(1)-P(2A)	91.8(2)
P(2)-Sn(1)-P(3)	92.83(8)	P(2)-Rb(1)-P(2A)	55.03(7)
Sn(1)-P(2)-P(1)	83.66(9)	P(3)-Rb(1)-P(2)	
P(3)-H(3P)-O(1S)	67.48(7) 156(1)		

[a] Symmetry transformations used to generated equivalent atoms labelled A: x, y, $-z$.

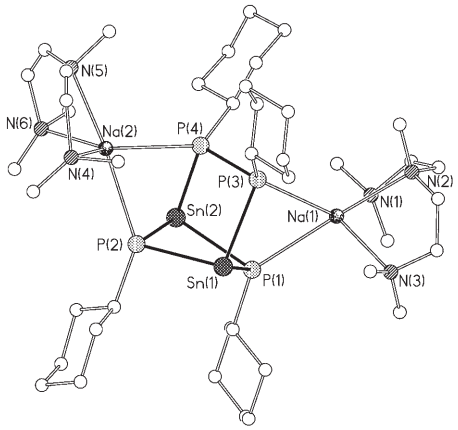

Figure 2. Structure of (Na·PMDETA)$_2$[{Sn(μ-PCy)}$_2$(μ-CyPPCy)] (**4**). Hydrogen atoms and lattice-bound toluene molecules have been omitted for clarity.

from their Sn_2P_4 cores. The acute P-Sn-P angles in **2** and **4** also suggest that a high degree of Sn p-character is present in the Sn−P bonds. The primary reason for the distortion of Sn^{II} geometry in both complexes is the coordination of their [{Sn(μ-PR)}$_2${μ-P(R)P(R)}]$^{2-}$ dianions to the two alkali metal cations, using one of the P centres of the RP–PR group and a bridging RP ligand. This chelation results in compression of the associated P-Sn-P angles below 90° (i.e., P(1)-Sn(1)-P(3) and P(2)-Sn(2)-P(4) mean 78.5° in **4**; cf. mean 75.8° for the corresponding angles in **2**).[5] Also similar to the previously reported complex **2**, is the P−P bond length within the CyP–PCy unit of the dianion of **4** (P(3)−P(4) 2.194(4) Å; cf. 2.186(2) Å in **2**).[5] This bond length is

 © 2007 Wiley-VCH Verlag GmbH & Co. KGaA, Weinheim

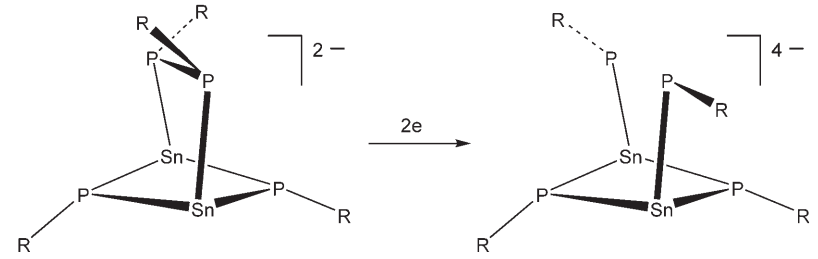

Scheme 5.

shorter than normally expected for a single P–P bond (ca. 2.21 Å),[9] presumably as a result of the bridging of the CyP–PCy ligand across the Sn_2P_2 ring of the dianion. The Sn–P[8,10] and Sn–Na[11] bond lengths in **4** are similar to those found in previously reported complexes.

The structure of **5** shows that the major component in the crystal is the bis-diphosphido complex $(K{\cdot}2THF)_2[Sn_2(\mu\text{-}PCyPCy)_2(\mu\text{-}PCy)]$ (**5a**) (Figure 3a). However, there is also evidence of a minor component which is interpreted as being due to 10% of a co-crystallised molecule in which one of the two CyP–PCy groups present in **5** is replaced by a single CyP ligand (Figure 5b) (see Experimental Section). The structure of the Sn^{II} bis-monophosphide anion of this component appears to be the same as that in molecules of $(Na{\cdot}PMDETA)_2[\{Sn(\mu\text{-}PCy)\}_2(\mu\text{-}PCyPCy)]$ (**4**) (Figure 2), thus formulating the contaminant as $(K{\cdot}2THF)_2[\{Sn(\mu\text{-}PCy)\}_2(\mu\text{-}PCyPCy)]$ (**5b**). The structure of the major component **5a** is an ion-paired species $(K{\cdot}2THF)_2[Sn_2(\mu\text{-}PCyPCy)_2(\mu\text{-}PCy)]$, resulting from the association of the $[Sn(\mu\text{-}PCyPCy)_2(\mu\text{-}PCy)]^{2-}$ dianion with two bis-solvated K^+ ions. The dianion units of the complex represents a completely new structural arrangement for a Sn^{II} phosphide, being composed of two crystallographically independent Sn^{II} centres that are bridged by two CyP–CyP groups and by one PCy group. The two K^+ ions within the molecular units of **5a** exhibit different coordination modes. K(1) is chelated by two P centres from separate CyP–PCy groups (K(1)–P(1) 3.290(2), K(1)–P(3) 3.438(2) Å), whereas K(2) is coordinated by the P centre of the bridging PCy group (K(2)–P(5) 3.280(2) Å) and by a P centre of a CyP–PCy group (K(2)–P(4) 3.353(2) Å). The presence of two distinct coordination modes for the K^+ ions clearly has a major effect on the overall geometry of the $[Sn(\mu\text{-}PCyPCy)_2(\mu\text{-}PCy)]^{2-}$ dianion, and is responsible for the relatively broad range of Sn–P bond lengths found within the Sn_2P_6 core (2.573(1)–2.615(2) Å).[12] However, the most obvious effect of this coordination is seen in the geometries of the Sn^{II} centres. The Sn(1) centre exhibits a more regular pyramidal geometry (P-Sn-P 91.35(6)–99.60(6)°) than that of Sn(2) (P-Sn-P 81.58(2)–105.46(5)°). The marked compression of the P(4)-Sn(2)-P(5) angle (81.59(5)°) stems from the chelation of K(2) by P(4) and P(5). A closely related effect was noted above in the structures of **2** and **4**, where a similar metal-coordinating mode is found, involving one of the RP-PR P centres and the μ-CyP group. The involvement of both of the P centres of one of the CyP–PCy ligands in **5a** in the coordination of the two K^+ ions leads to a pronounced elongation of the P–P bond (P(3)–P(4) 2.214(2) Å) in this ligand compared to the other CyP–PCy ligand (P(1)–P(2) 2.200(2) Å).

A further feature of the structure of **5a** is the association of the molecular units into a polymeric arrangement in the crystal lattice, through Sn–K interactions involving both the Sn centres (Sn(1)–K(1C) 3.725(2), Sn(2)–K(2A) 3.674(2) Å) (Figure 4). These interactions result in a five-coordinate geometry for K(1) and a distorted tetrahedral geometry for K(2).

The X-ray crystallographic study of **6**·THF shows it to be the ion-paired species [Rb·PMDETA-$\{(CyP)_3SnP(H)Cy\}$]·THF, containing a heterocyclic $[(CyP)_3SnP(H)Cy]^-$ ion (Figure 5). This anion is disordered across a crystallographic mirror plane, through Sn(1), Rb(1),

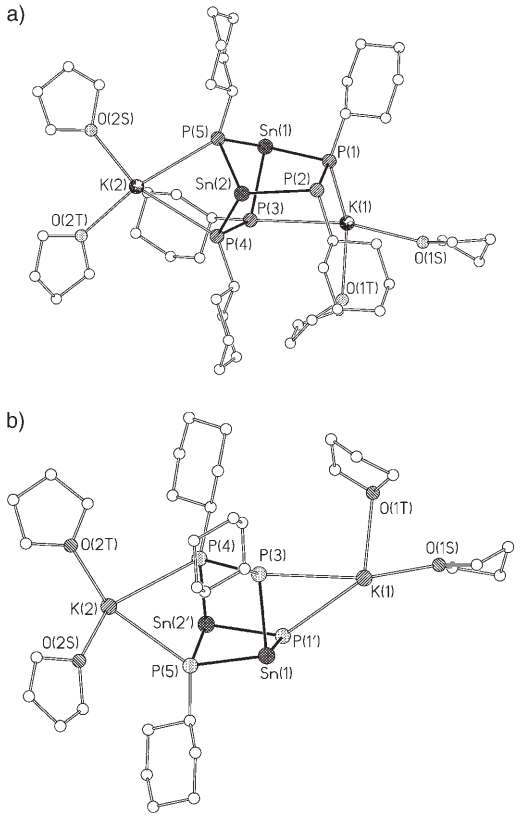

Figure 3. a) Structure of $(K{\cdot}2THF)_2[Sn_2(\mu\text{-}PCyPCy)_2(\mu\text{-}PCy)]$ (**5**), the major component (90%) in the crystals of **5**; b) proposed structure of the minor component in the crystals of **5** attributed to a 10% co-crystallisation of $(K{\cdot}2THF)_2[\{Sn(\mu\text{-}PCy)\}_2(\mu\text{-}PCyPCy)]$ (the carbon atoms of the cyclohexyl ring assumed to be bonded to P(1′) were not detected). Hydrogen atoms have been omitted for clarity.

 © 2007 Wiley-VCH Verlag GmbH & Co. KGaA, Weinheim

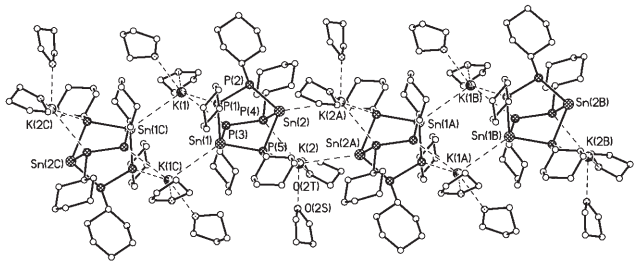

Figure 4. Association of units of the major component of **5** (**5a**) into a polymeric structure through Sn···K bonding. Hydrogen atoms and lattice-bound toluene molecules have been omitted for clarity.

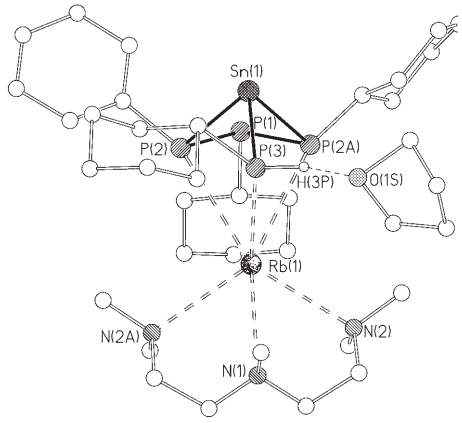

Figure 5. Structure of [Rb·PMDETA{(CyP)$_3$SnP(H)Cy}]·THF (**6**·THF).

P(3), and N(1) in the solid state. The Cy group attached to P(3), H(3) and a THF ligand (O1S–C4S), H-bonded the H(3P) occur with 50% occupancy on either side of the molecular mirror plane. Thus, both enantiomers of **6**·THF are randomly distributed over all equivalent positions in the crystal. The cyclic anion arrangement of **6**·THF is of particular interest, being analogous to the Group 15 anions $[(RP)_3As]^-$ (R = 1-adamantyl, *t*Bu).[4] Like the latter, the $[(CyP)_3SnP(H)Cy]^-$ ion is folded (by an angle of 53.5° about the Sn(1)···P(1) vector), and the Cy groups adopt an all-*trans* conformation with respect to the ring on steric grounds. The geometry of the Sn^{II} centre in **6**·THF is highly distorted (P-Sn-P 74.7(1)–92.7(1)°), with the smallest of the P-Sn-P angles being found within the P_3Sn ring unit. The coordination of the $[(CyP)_3SnP(H)Cy]^-$ ion to the Rb^+ ion involves both the Sn-bonded P centres of the P_3Sn ring unit (Rb(1)–P(2,2A) 3.431(3) Å) and the terminal PHCy P centre (Rb(1)–P(3) 3.362(5) Å). The Rb–P distances involved are typical of those found previously in Rb–P bonded complexes (3.34–3.84 Å).[12b,k,13,14]

Theoretical studies: As noted in the introduction to this paper, the $[\{Sn(\mu\text{-}PCy)\}_3]^{2-}$ dianion of **3** (Figure 1) is electron-deficient.[6] The relatively short Sn–Sn distances (3.1502(3)–3.1981(3) Å[6]) suggest that Sn–Sn bonding is present in this species. These Sn–Sn distances are within the range of values found in Sn–Sn-bonded complexes (mean 2.91 Å)[9] and are typical of Sn–Sn bond lengths present in electron-deficient Zintl ions such as Sn_5^{2-} and Sn_9^{4-}.[15] These distances are, however, longer than those found in compounds containing Sn=Sn double (2.77–2.83 Å),[17] or Sn···Sn partial (2.782(1)–2.824(1) Å)[17] multiple bonds. The acute Sn-P-Sn (75.55(2)–76.91(2)°) and P-Sn-P (93.10(3)–97.71(3)°) bond angles within the $[\{Sn(\mu\text{-}PCy)\}_3]^{2-}$ dianion are consistent with only limited hybridisation of the s and p orbitals on both the P and Sn centres.[6] Thus, a valence-bond interpretation of the bonding within the Sn_3 triangle of this dianion involves the overlap of three Sn p orbitals above the Sn_3 plane, forming a 2e-3c bonding system in which the Sn–Sn bond order is $^1/_3$ (Figure 6a). Alternatively,

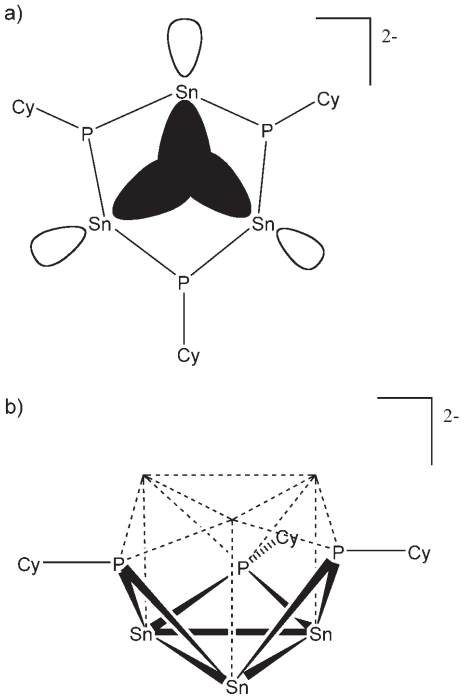

Figure 6. a) Valence-bond description of the anion of **3** (assuming unhybridised s and p orbitals on Sn); b) *hypho*-cluster model based on Wade's rules.

however, the structure of the $[Sn(\mu\text{-}PCy)]_3^{2-}$ dianion can be regarded as a *hypho*-cluster derived from a tricapped-trigonal prism in which three vertices are missing (i.e., with 6 vertices (n) and 10 ($n+4$) electron pairs involved in skeletal bonding; Figure 6b).[18] These bonding descriptions are the same as those proposed previously for the *tris*-homoaromatic dianions of 1,3,5-triboracyclohexane, of the type $[R'B(\mu\text{-}C(R)H)]_3^{2-}$,[19] which are isolelectronic with the dianion of **3**. Two complementary computational methods were used to examine the bonding in **3**, namely natural bond order (NBO) analysis and electron localisation function (ELF) calculations.

 © 2007 Wiley-VCH Verlag GmbH & Co. KGaA, Weinheim

NBO analysis of the bonding in 3: Model ab initio MO calculations of the isolated $[Sn(\mu\text{-}PR)]_3^{2-}$ dianion and the neutral complex $[Sn(\mu\text{-}PR)]_3Na_2$ were used to probe the bonding present in **3**.[20] The R ligand was varied to note the effect of the changes in the geometry and bonding within the framework of the dianion and neutral structures. Three ligands were used in this analysis, hydrogen, methyl and cyclohexyl groups. In the geometry optimisations for both the neutral and dianion species, a C_{3v}-symmetric structure was found to be a minimum at the Hartree–Fock (HF) and density functional theory (DFT) level when R = H and CH_3, whilst for R = C_6H_{11}, C_1 symmetry was assigned to the dianion and neutral structures. The optimised structures of the dianion and neutral complex at the HF and DFT (MPW1K and B3LYP) levels are in good agreement with the solid-state structure of **3** (Figure 1), particularly bearing in mind the lack of solvation of the Na^+ ions in the neutral complex (see Supporting Information).

Natural bond orbital (NBO) analysis was performed on the B3LYP wavefunction[26,27] based on the dianion and neutral optimised structures using the aug-cc-pvtz and cc-pvtz basis sets, respectively. NBO population analysis indicates a slight positive charge on Sn in both the neutral and dianion models, with significant negative charge residing on both P and R-group components in both (Table 4), with the exception being the hydrogen isomer where the R group cannot support a large negative charge. The residual distribution of the negative charge is contained on phosphorus when R = H. At the B3LYP level, the net charge donated from Na to the "dianion" component in the neutral molecule is in the range −1.528 to −1.552 for the various R groups. The NBO analysis of the neutral complex and dianion indicates the existence of a 2e–3c Sn_3 bond. The occupancy for the 2e–3c NBO in the dianion is in the range 1.976 to 1.988, whereas in the neutral molecule the occupancy drops within the range 1.801 to 1.817. The cyclohexyl model has the highest occupancy within the neutral structure and the lowest occupancy of the 2e–3c bond within the dianion. The character of the 2e–3c NBO is primarily constructed from *p* natural atomic orbitals (NAO) on Sn, each Sn contributing $^1/_3$ of a bond to this NBO. This NBO has the highest doubly occupied NBO energy and can be compared to the HOMO molecular orbital found in the neutral complex and dianion (Figure 7). Associated with this bonding 2e–3c NBO are two degenerate, antibonding Sn_3 NBOs. These antibonding NBOs play an important role in delocalisation of charge within the dianion, having a combined occupancy in the range 0.204 to 0.214 for the neutral species and 0.178 to 0.238 in the dianion (coming mostly from donation from the Sn–P NBOs). These antibonding NBOs can be regarded as the LUMOs within the molecular orbital framework. Each Sn forms two doubly occupied (2e–2c) NBOs with the nearest P centres, with occupancy around 1.92. These orbitals comprise 30% Sn and 70% P character, based on p-NAO character interactions. Based on the natural hybrid directional analysis of the Sn–P NBOs, there is considerable strain on these bonding orbitals when comparing the deviation of the Sn and P natural hybrid p orbitals from the Sn–P bond axes. The NBO analysis also shows that the lone pair orbitals on Sn are primarily s orbitals and those on P are sp orbitals (Table 5).

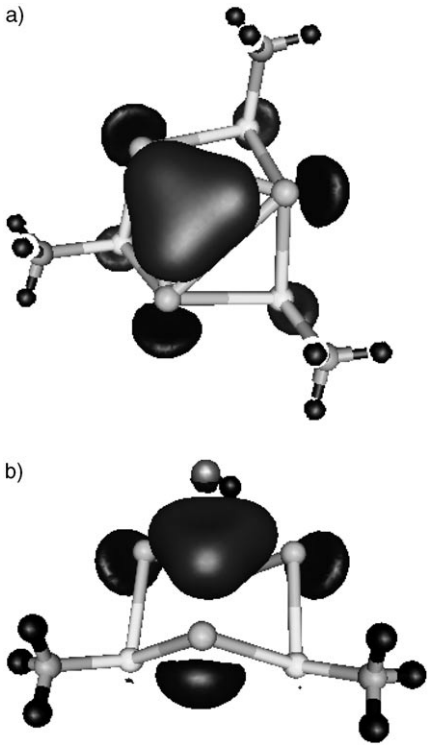

Figure 7. DFT(B3LYP)/cc-pvtz calculations of the HOMO of a) the discrete $[\{Sn(\mu\text{-}PMe)\}_3^{2-}$ dianion, and b) the neutral $[\{Sn(\mu\text{-}PMe)\}_3]Na_2$ molecule.

Table 5. Natural charge population analysis.

Molecule	Sn	P	R group	Na(1)[a]	Na(2)[b]
$[Sn(\mu\text{-}PCy)]_3Na_2$	0.151	−0.431	−0.235	0.859	0.687
$[Sn(\mu\text{-}PCy)]_3^{2-}$	0.037	−0.338	−0.366	–	–
$[Sn(\mu\text{-}PMe)]_3Na_2$	0.149	−0.429	−0.229	0.858	0.670
$[Sn(\mu\text{-}PMe)]_3^{2-}$	0.068	−0.406	−0.329	–	–
$[Sn(\mu\text{-}PH)]_3Na_2$	0.194	−0.744	−0.033	0.878	0.674
$[Sn(\mu\text{-}PH)]_3^{2-}$	0.062	−0.672	−0.056	–	–

[a] Na bonded to Sn. [b] Na bonded to P.

Electron localisation function (ELF) calculations on 3: Topological analysis of the electron localisation function (ELF) was employed to gain further insight into the chemical bonding in the $[Sn(\mu\text{-}PCy)]_3^{2-}$ dianion by calculating the electron populations, their variances and the covariance of the ELF basins, that is, essentially how the electron densities present in the orbitals relate to each other.[28] Ab initio calculations were performed using Gaussian03 at the HF level of theory with 6–311++G(3dp,3df) as the basis set for P, Na, C and H atoms, and 3–21G(d, p) for the Sn atoms.[29] In all the calculations, a singlet state was assumed and the Hesse matrices were checked for the absence of imaginary

 © 2007 Wiley-VCH Verlag GmbH & Co. KGaA, Weinheim

entries in geometry optimisations. A single-point wavefunction was calculated for $Na_2[Sn(\mu\text{-}PCy)]_3$ using the atomic coordinates obtained from the crystal structure of **3**, and geometry optimisations of the isolated $[Sn(\mu\text{-}PH)]_3^{2-}$ dianion and $Na_2[Sn(\mu\text{-}PH)]_3$ in point group C_{3v} were also performed. The calculation of the ELF was done using TopMod.[30] Since the results are essentially the same for the three species, only the results for the free dianion $[Sn(\mu\text{-}PH)]_3^{2-}$ are presented here. Figure 8 shows the reducible localisation

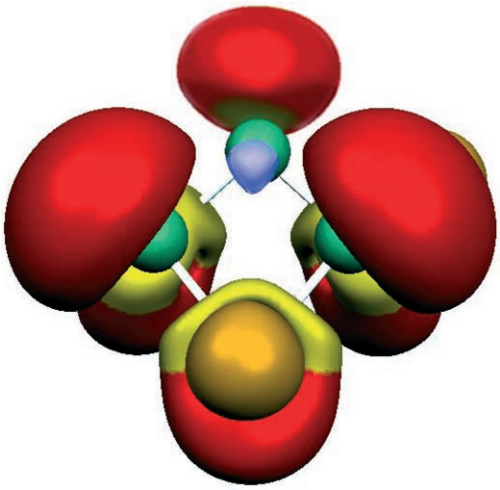

Figure 8. The reducible localisation domains of the ELF of the $[Sn_3(\mu\text{-}PH)]_3^{2-}$ dianion (C_{3v}) at $\eta(r)=0.70$, viewed along a vertical mirror plane with a hydrogen atom pointing toward the viewer. Core basins are green, monosynaptic valence basins (lone pairs) are red, protonated basins are orange, disynaptic basins are yellow and trisynaptic basins are blue.

domain of the electron localisation function of the $[Sn(\mu\text{-}PH)]_3^{2-}$ dianion at $\eta(r)=0.70$. Each of the three P core basins C(P) is populated by 9.97 electrons, with a variance of 0.44, which shows the delocalisation of the electrons.[28,31] The population of 9.97 electrons is very close to the expected ten electrons for the phosphorus core shell. Both values agree well with previous findings in P species, like P_6H_8, P_4, P_7^{3-}, P_{11}^{3-}, P_5^- and P_4^{2-}.[32–34] The covariance matrix contains information concerning the delocalisation of electrons between neighbouring basins. The covariance of the P core basins C(P) shows that the protonated disynaptic valence basin V(P, H) (the P–H bond, orange in Figure 8), the monosynaptic valence basin V(P) (the P lone pair, red) and the disynaptic valence basin V(P, Sn) (P–Sn bond, yellow) are involved in this delocalisation. The protonated disynaptic valence basin V(P, H) shows a population of 2.03 electrons with a higher variance of 0.67—delocalisation of electrons occurs between this protonated basin V(P, H) and its corresponding P core basin C(P) and monosynaptic valence basin V(P), and its corresponding disynaptic valence basins V(Sn, P), as is to be expected. The monosynaptic valence basin V(P) is populated by 2.35 electrons with a variance of 1.06 with major delocalisation between it and its corresponding core basin C(P), its protonated disynaptic valence basin V(P, H), its disynaptic valence basin V(P, Sn), but also between it and the neighbouring monosynaptic valence basins of the Sn atoms V(Sn). There is only very little delocalisation between the neighbouring monosynaptic valence basins of the P atoms.

The Sn core basin C(Sn) (Figure 8, green) is populated by 45.73 electrons with a rather high variance of 1.17, which is close to the expected value of 46 electrons for the core shell of tin. Delocalisation occurs mainly between the C(Sn) and the V(Sn) on the same Sn atom, between C(Sn) and the V(P, Sn) but also between it and the trisynaptic valence basin V(Sn, Sn, Sn) (colour-coded blue) to a minor extent. The disynaptic valence basin V(P, Sn) has a population of 1.77 electrons with a variance of 1.06, and delocalisation occurs between the neighbouring core basins, the neighbouring protonated monosynaptic valence basin V(P, H), to the lone pairs of the neighbouring phosphorus V(P) and tin atoms V(Sn), but also to the trisynaptic valence basin V(Sn, Sn, Sn) to a minor extent. The lone pairs on the Sn atoms show a population of 2.58 electrons with a rather high variance of 1.36. The covariance shows that the delocalisation occurs mainly between the V(Sn) and its corresponding C(Sn) and its neighbouring V(P, Sn). Some minor delocalisation occurs between it and its neighbouring V(P, H), V(P) and V(Sn). Consequently, no lone pair aromaticity is observed for this compound, for which delocalisation would have to occur mainly between the Sn lone pairs.[33] However, there is a pronounced and rather high delocalisation between the Sn lone pair and the trisynaptic valence basin V(Sn, Sn, Sn), which may readily be compared to the trisynaptic valence basins of hydro-*closo*-borates like $B_6H_6^{2-}$ or $B_{12}H_{12}^{2-}$. The population of this trisynaptic valence basin is 1.34 electrons, with a variance of 0.98. For comparison, the so-called 2e–3c bonds in the hydro-*closo*-borates $B_6H_6^{2-}$ and $B_{12}H_{12}^{2-}$ show populations of 1.60 and 1.22 electrons, with variances of 0.95 and 0.81, respectively.[35] Thus, the bond between the three tin atoms is similar to the bond between three boron atoms in hydro-*closo*-borates.

Although the absolute values of electron populations obtained from NBO and ELF methods are different, these calculations provide a consistent and mutually supportive view of the structure of the anion of **3**, showing the existence of a "borane-like" (formal) 2e–3c bond between the three Sn centres.

Closing Remarks

The studies of the reactions of $Sn(NMe_2)_2$ with CyPHM presented show that an extensive range of new Sn^{II} phosphinidene frameworks can be obtained. There is a strong dependence of these cage frameworks on the alkali metal and a broad tendency for increased formation of P–P and Sn–Sn bonding for the heavier alkali metals (M). This pattern is qualitatively similar to that found in the analogous reactions of the Group 15 reagents $[E(NMe_2)_3]$ with a range of primary phosphido alkali metal compounds. However, a

 © 2007 Wiley-VCH Verlag GmbH & Co. KGaA, Weinheim

number of questions still remain to be answered; specifically, 1) is there a common mechanism which is responsible for all of the Sn^{II} phosphinidene frameworks observed so far? and 2) what is the role played by the alkali metal in these reactions? There is emerging evidence of a mechanistic link between the metallacyclic tetraanion $[\{Sn(\mu\text{-}PR)\}_2(\mu\text{-}PR)]_2^{4-}$ and the $[\{Sn(\mu\text{-}PR)\}_2(\mu\text{-}PRPR)]^{2-}$ dianion. This connection can be understood by the proposed mechanism shown in Scheme 6.

Support for this mechanism comes the recent observation that the reaction of $Sn(NMe_2)_2$ with MesPHNa gives the unusual stannate trianion $[Sn\{(CH_2)4,6\text{-}Me_2C_6H_3P\}(PMes)]^{3-}$ in which deprotonation of a methyl substituent of a Mes group has occurred from the intermediate $[Sn(PMes)_2]^{2-}$ (a species of type **A**, Scheme 6).[36] This and other recent observations[37] suggest that the main reason for the difference in the outcomes of the reactions involving heavier alkali metals is the greater basicity and nucleophilicity of the RPH^- ions (i.e., arising from the greater polarity of P–M (M = Na–Rb) bonds compared to P–Li bonds). With this insight, the formation of the $[\{Sn(\mu\text{-}PCy)\}_2(\mu\text{-}PCyPCy)]^{2-}$ dianion within the major component of **5** can be explained by the nucleophilic attack of CyPHK on to an intermediate $[\{Sn(\mu\text{-}PCy)\}_2(\mu\text{-}PCyPCy)]^{2-}$ dianion (Scheme 7). Indeed, the latter species is apparently present as the minor component in the structure of **5**. ^{31}P NMR spectroscopic and theoretical studies are planned in order to test the proposed mechanisms (Scheme 5 and Scheme 6) and to understand how the frameworks of $[(Na\cdot PMDETA)_2\{Sn(\mu\text{-}PCy)\}_3]$ (**3**) and $[Rb\cdot PMDETA\{(CyP)_3SnP(H)Cy\}]$ (**6**) are formed.

Finally, NBO and ELF calculations of the trianion of **3** support the existence of Sn···Sn bonding, and a structure involving a formal 2e–3c bond between the three Sn centres.

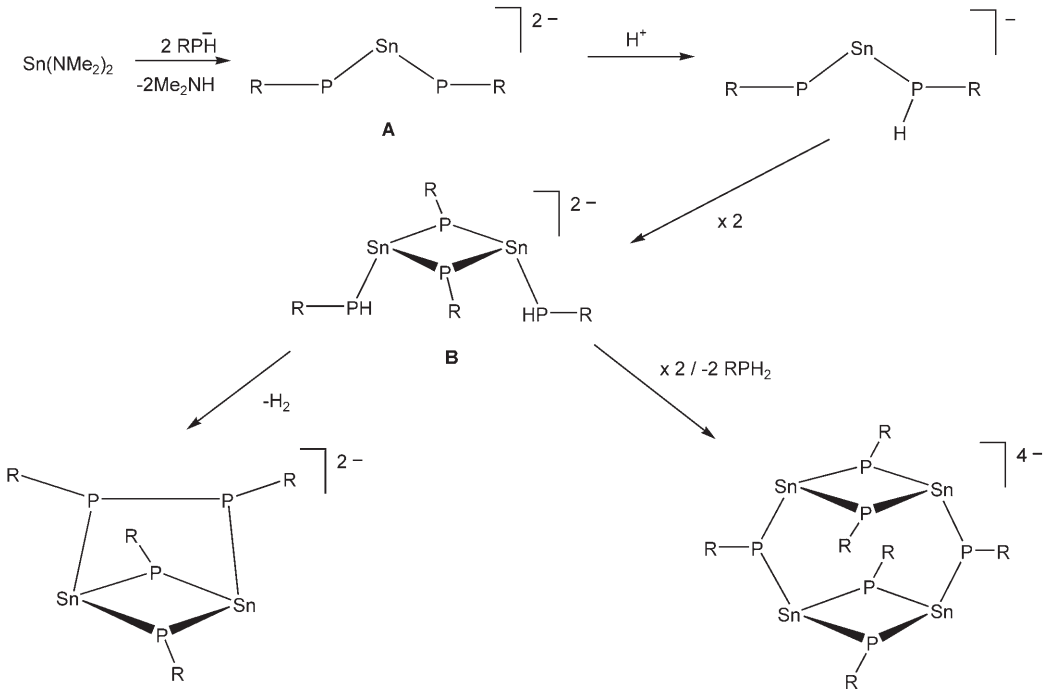

Scheme 6. Proposed mechanism linking the $[\{Sn(\mu\text{-}PR)\}_2(\mu\text{-}PR)]_2^{4-}$ tetraanion and the $[\{Sn(\mu\text{-}PR)\}_2(\mu\text{-}PRPR)]^{2-}$ dianion.

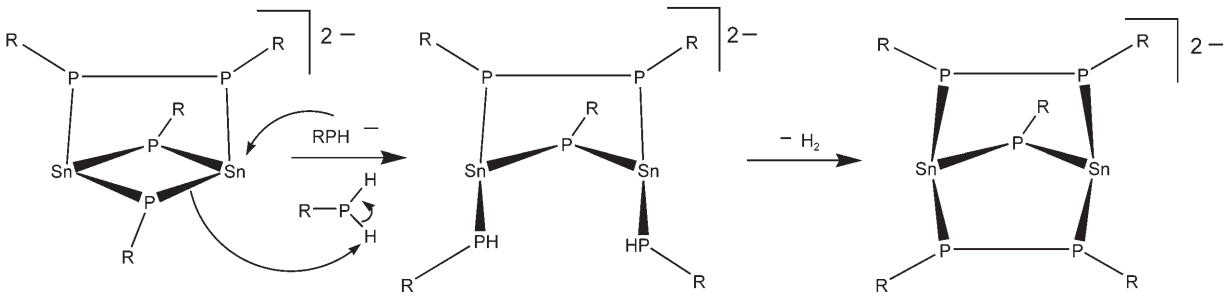

Scheme 7. Proposed mechanism of insertion of an RP group into the framework of the $[\{Sn(\mu\text{-}PR)\}_2(\mu\text{-}PRPR)]^{2-}$ dianion.

 © 2007 Wiley-VCH Verlag GmbH & Co. KGaA, Weinheim

Experimental Section

General: Compounds **4**, **5** and **6**·THF are air- and moisture-sensitive. They were handled on a vacuum line (in an efficient cupboard) using standard inert-atmosphere techniques and under dry/oxygen-free argon. $Sn(NMe_2)_2$ was prepared by using the literature route, by transmetalation of $SnCl_2$ with $LiNMe_2$ (1:2 equiv) in Et_2O.[38] It is stable if stored at −10 °C under argon for prolonged periods. $CyPH_2$ was acquired from the Aldrich Chemical Company and was used as supplied. THF, toluene, diethyl ether and hexane solvents were dried by distillation over sodium/benzophenone prior to the reactions. PMDETA (Aldrich) was dried by distillation over Na and stored over molecular sieves under argon. The products were isolated and characterised with the aid of an nitrogen-filled glove box fitted with a Belle Technology O_2 and H_2O internal recirculation system. Melting points were determined by using a conventional apparatus and sealing samples in capillaries under argon. IR spectra were recorded as Nujol mulls using NaCl plates and were run on a Perkin-Elmer Paragon 1000 FTIR spectrophotometer. Elemental analyses were performed by first sealing the samples under argon in air-tight aluminium boats (1–2 mg), and then the C, H and N content was analysed using an Exeter Analytical CE-440 Elemental Analyser. ^1H, ^{31}P and ^{119}Sn NMR spectra were recorded on a Bruker DPX 400 MHz spectrometer in dry THF or DMSO (using the solvent resonances as the internal reference standard). The synthesis of **3** was described in reference [6].

Synthesis of 4: A suspension of $NaCH_2Ph$ (0.62 g, 8.5 mmol) in toluene (80 mL) was cooled to −78 °C. $CyPH_2$ (0.67 mL, 8.5 mmol) was added to the suspension and the mixture was allowed to reach room temperature. A bright yellow suspension of NaPHCy was formed after stirring (12 h). A suspension of $Sn(NMe_2)_2$ (1.54 g, 8.5 mmol) in toluene (20 mL) was then added to the metalated phosphine at −78 °C. The mixture became orange in colour and, after stirring at room temperature overnight, a red suspension in a red solution was formed. PMDETA (excess, 4.0 mL) was added slowly to dissolve most of the red solid. The mixture was then filtered through celite and the solution reduced in volume to about 20 mL under vacuum. Storage at room temperature (2 h) gave orange crystals of **1** contaminated with **4** (as shown by X-ray analysis and unit cell determinations of several crystals).

Synthesis of 5: A suspension of KCH_2Ph (2.0 g, 15.36 mmol) in toluene (50 mL) was cooled at −78 °C. $CyPH_2$ (1.7 mL, 12.8 mmol) was added to the suspension and the mixture stirred until it reached room temperature. Stirring was continued for 12 h. A brown suspension was produced. A suspension of $Sn(NMe_2)_2$ (1.44 g, 6.98 mmol) in toluene (20 mL) was added to this suspension at −78 °C. The colour changed to red when the reaction mixture reached room temperature. Stirring was continued overnight. The toluene was removed and the most of the red-orange precipitate produced was dissolved in THF. Filtration followed by the addition of Et_2O (5 mL) gave a clear orange solution that was stored at −20 °C (24 h) to give orange crystals of **5**. M.p. 130 °C (decomp). Yield 0.40 g (10%, based on Sn supplied). ^1H NMR ([D_8]THF, 25 °C, 500.16 MHz): $\delta = 3.68$ (m, THF), 2.6–1.0 (m, 11 H), 1.52 ppm (m, THF); ^{31}P NMR ([D_8]THF, 25 °C, 161.975 MHz): $\delta = -127.0$ to −222.2 ppm; ^{119}Sn NMR ([D_8]THF, 25 °C, rel. to $SnCl_2/D_2O$): $\delta = -1540.0$ ppm (s); elemental analysis calcd (%) for **5**·8 THF: C 40.6, H 6.3, P 16.3; found: C 42.9, H 6.9, P 17.2.

Synthesis of 6: A suspension of $RbCH_2Ph$ (0.50 g, 2.83 mmol) in toluene (50 mL) was cooled at −78 °C. $CyPH_2$ (0.35 mL, 2.6 mmol) was added to the suspension and the mixture was stirred until it reached room temperature. Stirring was continued for 12 h. $Sn(NMe_2)_2$ (0.18 g, 0.86 mmol) and PMDETA (5 mL) were added, which produced a red solid in an orange solution. The solvent was removed and replaced by THF (50 mL). The solid was filtered off and the filtrate was reduced in volume (to ca. 10 mL). Storage at −15 °C for 48 h gave colourless blocks of **6**. Yield 0.02 g (3%). ^{31}P NMR (THF, 25 °C, 161.95 MHz): $\delta = 74.0$ (t, P(1)), −3.4 (t, P(3)), −10.7 ppm (dd, $J_{P(2),P(3)} = 87.6$ Hz, $J_{P(2),P(1)=} 162.0$ Hz; P(2)). ^{31}P NMR spectroscopic studies of the crude powder show that this is almost all **6**, contaminated by traces of $[CyP]_4$. The yield of the powder (before filtering the suspension in THF in order to grow crystals) is almost quantitative with respect to Sn (ca. 0.55 g obtained; 0.58 g expected on the basis of Sn supplied (94%)). ^{31}P NMR studies showed that this powder consists of **6** contaminated with $[CyP]_4$.

X-ray studies on 4–6: Crystals of **4**, **5** and **6** were mounted directly from solution under argon using an inert oil to protect them from atmospheric oxygen and moisture. X-ray intensity data were collected by using a Nonius Kappa CCD diffractometer. Selected crystal and structure refinement data are given in Table 1. The three structures were solved by direct method and refined by full-matrix least-squares on F^2.[39] Crystals of **4**·1.5 toluene diffracted very weakly at high angle, data being only obtained in a θ range to 17.38°. This may be explained by the considerable conformational disorder of the two PMDETA ligands, with some carbon atoms being resolved into two components of 50:50 occupancy, and the partial occupancy (50%) of the three toluene solvate sites in the asymmetric unit. The shortage of data resulted in relatively high esd values on the metric parameters, but despite this the important features of the molecule of **4** are well established. The crystal of **5** diffracted well despite some disorder of three of the four THF ligands, which was partially resolved in to components of about 50:50 occupancy (rings O(1S) and (O1T)) and 75:25 (ring O(2s)). Initial refinement resulted in large residual maxima in the final difference Fourier of about 4 e$Å^{-3}$ very near the metal centre Sn(2) and of 2 e$Å^{-3}$ near two phosphorus atoms P(1) and P(2), respectively. These were interpreted as being due to 10% of a co-crystallised molecule in which one of the two CyPPCy groups present in **5** was replaced by a single CyP ligand. Two atoms of site occupancy 0.1, Sn(2′) and P(1′), were therefore included in a satisfactory refinement in which the site occupancy of Sn(2), P(1), P(2) and the two associated Cy rings was reduced to 0.9 site occupancy. The 0.1 occupancy carbon atoms of the Cy ring attached to P(1′) could not be detected. However from the position of the P(1′) donor-bridging atom Sn(1) and Sn(2′), Sn(1)–P(1′) 2.47(1) and Sn(2′)–P(1′) 2.53(1) Å and the similarity of the partial structure (Figure 3b) to (Na·PMDETA)$_2$[{Sn(μ-PCy)}$_2$(μ-PCyPCy)] molecule **4** (Figure 2) it seems reasonable to deduce that the contaminant is the analogous molecule (K·2 THF)$_2$[{Sn(μ-PCy)}$_2$(μ-PCyPCy)], co-crystallised with most atoms in the two components overlapping. The third crystal **6**·THF showed extensive disorder due to a crystallographic mirror plane (through Sn(1), Rb(1), P(1), P(3) and N(1)) bisecting the chiral molecule. The Cy ring on P(3) has exact mirror symmetry, but that on P(2) occurs in two orientations of equal occupancy and some carbon atoms of the PMDETA ligand were resolved into two equal components indicating a lack of exact mirror symmetry in its conformation. The main structural disorder is the presence of two mirror symmetry related orientations for the P(HPCy) ligand, P(3) being on the mirror, and the THF solvate H-bonded to H(3P). Owing to the disorder, the crystal diffracted relatively weakly at high angle and data in the limited θ range 4.18 to 21.00° were used in the refinement, and a relatively high R_1 factor of 0.079 was obtained; however the principal structural features are well established. In the final cycles of refinement for all three structures hydrogen atoms were included in idealised positions, and anisotropic displacement parameters were assigned to all full-occupancy non-hydrogen atoms and to the 0.9 occupancy atoms in **5.** CCDC-606553 (**4**), CCDC-606554 (**5**) and CCDC-606555 (**6**) contain the supplementary crystallographic data for this paper. These data can be obtained free of charge from The Cambridge Crystallographic Data Centre via www.ccdc.cam.ac.uk/data_request/cif.

Acknowledgements

We gratefully acknowledge the EPSRC (A.D.B, F.G., G.T.L., C.M.P., M.McP., D.S.W.), The EU (Socrates Program, P.A., J.P.H.), The Cambridge European Trust (F.G.), St. Catharine's College, Cambridge (A.D.W.), the Deutsche Forschungsgemeinschaft (N.K., F.K.) and the Fonds der Chemischen Industrie (F.K.) for financial support. We also thank Dr. J. E. Davies (Cambridge) for collecting X-ray data for all compounds.

 © 2007 Wiley-VCH Verlag GmbH & Co. KGaA, Weinheim

[1] A. D. Hopkins, J. A. Woods, D. S. Wright, *Coord. Chem. Rev.* **2001**, *216*, 155; M. A. Beswick, C. N. Harmer, A. D. Hopkins, M. McPartlin, D. S. Wright, *Science* **1998**, *281*, 1500.

[2] M. A. Beswick, J. M. Goodman, C. N. Harmer, A. D. Hopkins, M. A. Paver, P. R. Raithby, A. E. H. Wheatley, D. S. Wright, *Chem. Commun.* **1997**, 1897.

[3] A. Bashall, F. García, G. T. Lawson, M. McPartlin, A. Rothenberger, A. D. Woods, D. S. Wright, *Can. J. Chem.* **2002**, *80*, 1421.

[4] a) M. A. Beswick, N. Choi, A. D. Hopkins, M. E. G. Mosquera, M. McPartlin, P. R. Raithby, A. Rothenberger, D. Stalke, A. E. H. Wheatley, D. S. Wright, *Chem. Commun.* **1998**, 2485; b) A. Bashall, M. A. Beswick, N. Choi, A. D. Hopkins, S. J. Kidd, Y. G. Lawson, M. E. G. Mosquera, M. McPartlin, P. R. Raithby, A. E. H. Wheatley, J. A. Wood, D. S. Wright, *J. Chem. Soc. Dalton Trans.* **2000**, 479.

[5] A. D. Bond, A. Hopkins, A. Rothenberger, A. D. Wood, D. S. Wright, *Chem. Commun.* **2001**, 525.

[6] P. Alvarez-Bercedo, A. D. Bond, A. D. Hopkins, G. T. Lawson, M. McPartlin, D. Moncrieff, J. M. Rawson, A. D. Woods, D. S. Wright, *Chem. Commun.* **2003**, 1288.

[7] For example, see: J.-P. Albrand, C. Taïeb, *Proceedings of the 1981 International Conference on Phosphorus Chemistry*, ACS Symposium Series, **1981**, *119*, 577.

[8] M. Westerhausen, W. Schwarz, *Z. Anorg. Allg. Chem.* **1996**, *622*, 903.

[9] Cambridge Crystallographic Data Base search (January 2006): F. H. Allen, O. Kennard, *Chem. Des. Autom. News* **1993**, *8*, 1.

[10] For examples, see: M. Westerhausen, R. Low, W. Schwarz, *J. Organomet. Chem.* **1994**, *513*, 213; R. E. Allan, M. A. Beswick, N. L. Chromhout, M. A. Paver, P. R. Raithby, M. Trevithick, D. S. Wright, *Chem. Commun.* **1996**, 1501; M. Driess, S. Martin, K. Merz, U. Pintchouk, H. Pritzkow, H. Grützmacher, M. Kaupp, *Angew. Chem.* **1997**, *109*, 1982; *Angew. Chem. Int. Ed. Engl.* **1997**, *36*, 1894; M. Krofta, N. Wiberg, H. Noth, A. Pfitzer, *Z. Naturforsch. B* **1998**, *53*, 1489.

[11] These values are typical of direct P-Na bonds, see for example: G. A. Koutsantonis, P. C. Andrews, C. L. Raston, *J. Chem. Soc. Chem. Commun.* **1995**, 47; O. Kuhl, J. Sieler, G. Baum, E. Hey-Hawkins, *Z. Anorg. Allg. Chem.* **2000**, *625*, 605.

[12] The K–P bonds in **5** are similar to those reported previously, a) M. Andrianarison, D. Stalke, U. Klingebiel, *Chem. Ber.* **1990**, *123*, 71; b) U. Englich, K. Hassler, K. Ruhlandt-Senge, F. Uhlig, *Inorg. Chem.* **1998**, *37*, 3532; c) C. Frenzel, P. Jorchel, E. Hey-Hawkins, *Chem. Commun.* **1998**, 1363; d) G. W. Rabe, S. Kheradmandan, G. P. A. Yap, *Inorg. Chem.* **1998**, *37*, 6451; e) M. A. Beswick, A. D. Hopkins, L. C. Kerr, M. E. G. Mosquera, P. R. Raithby, D. Stalke, A. Steiner, D. S. Wright, *Chem. Commun.* **1998**, 1527; f) O. Kuhl, J. Sieler, E. Hey-Hawkins, *Z. Kristallogr.* **1999**, *214*, 496; g) H. Karsch, V. W. Graf, M. Reisky, *Chem. Commun.* **1999**, 1695; h) W. Clegg, S. Doherty, K. Izod, H. Kagerer, P. O'Shaughnessy, M. Sheffield, *J. Chem. Soc. Dalton Trans.* **1999**, 1825; i) M. A. Beswick, A. Bashall, A. D. Hopkins, S. J. Kidd, Y. G. Lawson, M. McPartlin, P. R. Raithby, A. Rothenberger, D. Stalke, D. S. Wright, *Chem. Commun.* **1999**, 739; j) W. Clegg, K. Izod, P. O'Shaughnessy, *Organometallics* **1999**, *18*, 2939; k) G. W. Rabe, H. Heise, L. M. Liable-Sands, I. A. Guzei, A. L. Rheingold, *J. Chem. Soc. Dalton Trans.* **2000**, 1863; l) C. Frenzel, F. Somoza, Jnr. , S. Blaurock, E. Hey-Hawkins, *Chem. Commun.* **2001**, 3115.

[13] These Sn–K bond lengths are typical of previously reported compounds: T. F. Fässler, R. Hoffman, *Angew. Chem.* **1999**, *111*, 526; *Angew. Chem. Int. Ed.* **1999**, *38*, 543; P. B. Hitchcock, M. F. Lappert, G. A. Lawless, B. Royo, *J. Chem. Soc. Chem. Commun.* **1993**, 554.

[14] N. Korber, H. G. von Schnering, *Chem. Ber.*, **1996**, *129*, 155; J. Ellerman, W. Bauer, M. Schutz, F. W. Heinemann, M. Moll, *Monatsh. Chem.* **1998**, *129*, 547; G. W. Rabe, S. Kheradmandan, L. M. Liable-Sands, I. A. Guzei, A. L. Rheingold, *Angew. Chem.* **1998**, *110*, 1495; *Angew. Chem. Int. Ed.* **1998**, *37*, 1404; K. Izod, W. Clegg, S. T. Liddle, *Organometallics* **2001**, *20*, 367.

[15] J. D. Corbett, P. A. Edwards, *J. Chem. Soc. Chem. Commun.*, **1975**, 984; L. Dichl, K. Khodadadeh, D. Kummer, T. Strahle, *Chem. Ber.* **1976**, *109*, 3404; P. A. Edwards, J. D. Corbett, *Inorg. Chem.* **1977**, *16*, 903; J. D. Corbett, P. A. Edwards, *J. Am. Chem. Soc.* **1977**, *99*, 3313; M. Somer, W. Carrillo-Cabrera, E.-M. Peters, K. Peters, M. Kaupp, H.-G. von Schnering, *Z. Anorg. Allg. Chem.* **1999**, *625*, 37; R. Hauptmann, T. F. Fässler, *Z. Anorg. Allg. Chem.* **1999**, *627*, 2220.

[16] D. E. Goldberg, D. H. Harris, M. F. Lappert, K. M. Thomas, *J. Chem. Soc. Chem. Commun.* **1976**, 261; D. E. Goldberg, P. B. Hitchcock, M. F. Lappert, K. M. Thomas, A. J. Thorne, T. Fjeldberg, A. Haaland, B. E. R. Schilling, *J. Chem. Soc. Dalton Trans.* **1986**, 2387; K. W. Klinkhammer, T. F. Fässler, H. Grützmacher, *Angew. Chem.* **1998**, *110*, 114; *Angew. Chem. Int. Ed.* **1998**, *37*, 124; M. Sturman, W. Saak, K. W. Klinkhammer, M. Weidenbruch, *Z. Anorg. Allg. Chem.* **1999**, *625*, 1955.

[17] M. M. Olmstead, R. S. Simons, P. P. Power, *J. Am. Chem. Soc.* **1997**, *119*, 11705; L. Pu, S. T. Haubrich, P. P. Power, *J. Organomet. Chem.* **1999**, *582*, 100.

[18] K. Wade, *Adv. Inorg. Chem. Radiochem.* **1976**, *18*, 1; D. M. P. Mingos, *Adv. Organomet. Chem.* **1977**, *15*, 1.

[19] W. Lößlein, H. Pritzkow, P. von R. Schleyer, L. R. Schmitz, W. Siebert, *Angew. Chem.* **2000**, *112*, 1333; *Angew. Chem. Int. Ed.* **2000**, *39*, 1276.

[20] Geometry optimisations and frequency analyses were performed by using the Gaussian 98 software program.[21] In the neutral molecule a cc-pvtz[22] basis set was employed for all atoms excepted for tin, while an aug-cc-pvtz[22] basis set was employed in the dianion for all non-metallic atoms. An effective core potential was used to represent the core 46 electrons on the tin atom, a SDB-cc-pvtz[23] basis set was used on the neutral molecule, while a SDB-aug-cc-pvtz[23] basis set was used on the dianion for the tin atom. Two functionals were used in the DFT calculations, a B3LYP[24] functional and a MPW1K[25] functional. In both cases the INT = ULTRAFINE parameter was used to define the numerical grid.

[21] Gaussian 98, Revision A.11.2, M. J. Frisch, G. W. Trucks, H. B. Schlegel, G. E. Scuseria, M. A. Robb, J. R. Cheeseman, V. G. Zakrzewski, J. A. Montgomery, Jr., R. E. Stratmann, J. C. Burant, S. Dapprich, J. M. Millam, A. D. Daniels, K. N. Kudin, M. C. Strain, O. Farkas, J. Tomasi, V. Barone, M. Cossi, R. Cammi, B. Mennucci, C. Pomelli, C. Adamo, S. Clifford, J. Ochterski, G. A. Petersson, P. Y. Ayala, Q. Cui, K. Morokuma, N. Rega, P. Salvador, J. J. Dannenberg, D. K. Malick, A. D. Rabuck, K. Raghavachari, J. B. Foresman, J. Cioslowski, J. V. Ortiz, A. G. Baboul, B. B. Stefanov, G. Liu, A. Liashenko, P. Piskorz, I. Komaromi, R. Gomperts, R. L. Martin, D. J. Fox, T. Keith, M. A. Al-Laham, C. Y. Peng, A. Nanayakkara, M. Challacombe, P. M. W. Gill, B. Johnson, W. Chen, M. W. Wong, J. L. Andres, C. Gonzalez, M. Head-Gordon, E. S. Replogle, J. A. Pople, Gaussian, Inc., Pittsburgh PA, **2001**.

[22] T. H. Dunning, *J. Chem. Phys.* **1989**, *90*, 1007; R. A. Kendall, T. H. Dunning, R. J. Harrison, *J. Chem. Phys.* **1992**, *96*, 6769; D. E. Woon, T. H. Dunning, *J. Chem. Phys.* **1993**, *98*, 1358.

[23] J. M. L. Martin, A. Sundermann, *J. Chem. Phys.* **2001**, *114*, 3408; A. Bergner, M. Dolg, W. Kuechle, H. Stoll, H. Preuss, *Mol. Phys.* **1993**, *80*, 1431.

[24] A. D. Becke, *J. Chem. Phys.* **1993**, *104*, 1040.

[25] B. J. Lynch, P. L. Fast, M. Harris, D. G. Truhlar, *J. Phys. Chem. A* **2000**, *104*, 4811.

[26] R. J. Harrison, J. A. Nichols, T. P. Straatsma, M. Dupuis, E. J. Bylaska, G. I. Fann, T. L. Windus, E. Apra, W. de Jong, S. Hirata, M. T. Hackler, J. Anchell, D. Bernholdt, P. Borowski, T. Clark, D. Clerc, H. Dachsel, M. Deegan, K. Dyall, D. Elwood, H. Fruchtl, E. Glendening, M. Gutowski, K. Hirao, A. Hess, J. Jaffe, B. Johnson, J. Ju, R. Kendall, R. Kobayashi, R. Kutteh, Z. Lin, R. Littlefield, X. Long, B. Meng, T. Nakajima, J. Nieplocha, S. Niu, M. Rosing, G. Sandrone, M. Stave, H. Taylor, G. Thomas, J. van Lenthe, K. Wolinski, A. Wong, Z. Zhang, "NWChem, A Computational Chemistry Package for Parallel Computers, Version 4.1" (2002), Pacific Northwest National Laboratory, Richland, Washington 99352–0999, USA. T. P. Straatsma, E. Apra, T. L. Windus, M. Dupuis, E. J. Bylaska, W.

 © 2007 Wiley-VCH Verlag GmbH & Co. KGaA, Weinheim

de Jong, S. Hirata, D. M. A. Smith, M. T. Hackler, L. Pollack, R. J. Harrison, J. Nieplocha, V. Tipparaju, M. Krishnan, E. Brown, G. Cisneros, G. I. Fann, H. Fruchtl, J. Garza, K. Hirao, R. Kendall, J. A. Nichols, K. Tsemekhman, M. Valiev, K. Wolinski, J. Anchell, D. Bernholdt, P. Borowski, T. Clark, D. Clerc, H. Dachsel, M. Deegan, K. Dyall, D. Elwood, E. Glendening, M. Gutowski, A. Hess, J. Jaffe, B. Johnson, J. Ju, R. Kobayashi, R. Kutteh, Z. Lin, R. Littlefield, X. Long, B. Meng, T. Nakajima, S. Niu, M. Rosing, G. Sandrone, M. Stave, H. Taylor, G. Thomas, J. van Lenthe, A. Wong, and Z. Zhang, "NWChem, A Computational Chemistry Package for Parallel Computers, Version 4.5" (2003), Pacific Northwest National Laboratory, Richland, Washington 99352–0999, USA.

[27] NBO 5.0. E. D. Glendening, J. K. Badenhoop, A. E. Reed, J. E. Carpenter, J. A. Bohmann, C. M. Morales, and F. Weinhold (Theoretical Chemistry Institute, University of Wisconsin, Madison, WI, **2001**); http://www.chem.wisc.edu/~nbo5.

[28] a) A. D. Becke, K. E. J. Edgecombe, *J. Chem. Phys.* **1990**, *92* 5397; b) A. Savin, A. D. Becke, J. Flad, R. Nesper, H. Preuss, H. G. von Schnering, *Angew. Chem.* **1991**, *103*, 421; *Angew. Chem. Int. Ed. Engl.* **1991**, *30*, 409; c) B. Silvi, A. Savin, *Nature* **1994**, *371*, 683; d) T. Fässler, A. Savin, *Chem. unserer Zeit* **1997**, *31*, 110; e) A. Savin, R. Nesper, S. Wengert, T. F. Fässler, *Angew. Chem.* **1997**, *109*, 1892; *Angew. Chem. Int. Ed. Engl.* **1997**, *36*, 1808; f) S. Noury, F. Colonna, A. Savin, B. Silvi, *J. Mol. Struct.* **1998**, *450*, 59; g) J. K. Burdett, T. A. McCormick, *J. Phys. Chem. A* **1998**, *102*, 6366; h) S. Noury, X. Krokidis, F. Fuster, B. Silvi, *Comput. Chem. Eng. Computers & Chemistry* **1999**, *23*, 597; i) H. Grützmacher, T. F. Fässler, *Chem. Eur. J.* **2000**, *6* , 2317; j) B. Silvi, *Phys. Chem. Chem. Phys.* **2004**, *6* 256; k) B. Silvi, I. Fourré, M. E. Alikhani, *Monatsh. Chem.* **2005**, *136*, 855.

[29] M. J. Frisch, G. W. Trucks, H. B. Schlegel, G. E. Scuseria, M. A. Robb, J. R. Cheeseman, J. A. Montgomery, T. Vreven, Jr., K. N. Kudin, J. C. Burant, J. M. Millam, S. S. Iyengar, J. Tomasi, V. Barone, B. Menucci, M. Cossi, G. Scalmani, N. Rega, G. A. Petersson, H. Nakatsuji, M. Hada, M. Ehara, K. Toyota, R. Fukuda, J. Hasegawa, M. Ishida, T. Nakajima, Y. Honda, O. Kitao, H. Nakai, M. Klene, X. Li, J. E. Knox, H. P. Hratchian, J. B. Cross, V. Bakken, C. Adamo, J. Jaramillo, R. Gomperts, R. E. Stratmann, O. Yazyev, A. J. Austin, R. Cammi, C. Pomelli, P. Y. Ayala, K. Morokuma, G. A. Voth, P. Salvador, J. J. Dannenberg, V. G. Zakrzewski, S. Dapprich, A. D. Daniels, M. C. Strain, O. Farkas, D. K. Malick, A. D. Rabuck, K. Raghavachari, J. B. Foresman, J. V. Ortiz, Q. Cui, A. G. Baboul, S. Clifford, J. Cioslowski, B. B. Stefanov, A. Liashenko, P. Piskorz, I. Komaromi, R. L. Martin, D. J. Fox, T. Keith, M. A. Al-Laham, C. Y. Peng, A. Nanayakkara, M. Challacombe, P. M. W. Gill, B. Johnson, W. Chen, M. W. Wong, C. Gonzalez, C., J. A. Pople, Gaussian03, Revision C.02. 03 [Revision C.02], Wallingford CT, Gaussian, Inc, **2004**.

[30] S. Noury, X. Krokidis, F. Fuster, B. Silvi, *ToPMoD*, Laboratoire de Chimie Théorique (UMR-CNRS 7616) Université Pierre et Marie Curie, 75252 Paris cédex, France, **1997**.

[31] D. B. Chesnut, L. J. Bartolotti, *Chem. Phys.* **2000**, *253*, 1.

[32] F. Kraus, N. Korber, *Chem. Eur. J.* **2005**, *11*, 5945.

[33] F. Kraus, T. Hanauer, N. Korber, *Inorg. Chem.* **2006**, *45*, 1117.

[34] F. Kraus, T. Hanauer, N. Korber, *Angew. Chem.* **2005**, *117*, 7366; *Angew. Chem. Int. Ed.* **2005**, *44*, 7200.

[35] F. Kraus, B. Albert, unpublished results **2005**.

[36] M. McPartlin, A. D. Woods, C. M. Pask, T. Vogler, D. S. Wright, *J. Chem. Soc. Chem. Commun.* in **2003**, 1524.

[37] Similar reactions involving more sterically demanding *t*BuPHM do not result in P–P coupling, see: F. García, J. P. Hehn, R. A. Kowenicki, M. McPartlin, C. M. Pask, A. Rothenberger, M. L. Stead, D. S. Wright, *Organometallics*, in press.

[38] M. M. Olmstead, P. P. Power, *Inorg. Chem.* **1984**, *23*, 413.

[39] G. M. Sheldrick, SHELX-97, Göttingen, Germany, **1997**.

Received: May 5, 2006
Published online: November 6, 2006

 © 2007 Wiley-VCH Verlag GmbH & Co. KGaA, Weinheim